

fraction, can give nontrivial geometric information. Examples are the (known) relaxation of the GaAs(110) surface, and a detailed geometry of 2×1 H on Ni(110). Further tests of the potential, of soft-wall effects, and of other effects in diffraction are necessary to move towards more quantitative accuracy.

I would like to thank M. Cardillo, R. B. Laughlin, and T. Engle for helpful discussions.

¹For a recent review, see H. Hoinkes, *Rev. Mod. Phys.* **52**, 933 (1980).

²M. J. Cardillo and G. E. Becker, *Phys. Rev. Lett.* **42**, 508 (1979), and *Phys. Rev. B* **21**, 1497 (1980).

³M. Cardillo, G. E. Becker, S. J. Sibener, and D. R. Miller, to be published.

⁴K. H. Rieder and T. Engel, *Phys. Rev. Lett.* **45**, 824 (1980), and **43**, 373 (1979).

⁵R. B. Laughlin, to be published.

⁶N. Esbjerg and J. K. Nørskov, *Phys. Rev. Lett.* **45**, 807 (1980).

⁷J. A. Appelbaum and D. R. Hamann, *Phys. Rev. B* **6**, 2166 (1972).

⁸O. Jepsen, J. Madsen, and O. K. Andersen, *Phys. Rev. B* **18**, 605 (1978).

⁹D. R. Hamann (unpublished).

¹⁰E. P. Wigner, *Phys. Rev.* **46**, 1002 (1934). It is clear that the nonlocal image form is correct far from the surface. However, the wave functions are already strongly decaying at the local-image crossover point, and their shape is principally determined by the potential in the attractive region of the last atom layer, not by the nearly constant potential in the tail region.

¹¹N. Garcia, C. Ocal, and C. Prieto, to be published, find 0.0122 eV in a kinematic fit to bound-state resonances which neglects the corrugated wall.

¹²C. B. Duke, R. J. Meger, A. Paton, P. Mark, A. Kahn, E. So, and J. L. Yeh, *J. Vac. Sci. Technol.* **16**, 1252 (1979); B. J. Mrstik, S. Y. Tong, and M. A. Van Hove, *J. Vac. Sci. Technol.* **16**, 1258 (1979).

¹³G. R. Armand and J. R. Manson, *Phys. Rev. Lett.* **43**, 1839 (1979).

¹⁴R. B. Bau, W. E. Carroll, D. W. Hart, R. G. Teller, and T. F. Koetzle, in *Transition Metal Hydrides*, edited by R. Bau (American Chemical Society, Washington, D. C., 1978), p. 72.

Observation of Superlattice Effects on the Electronic Bands of Multilayer Heterostructures

E. E. Mendez, L. L. Chang, G. Landgren,^(a) R. Ludeke, and L. Esaki
IBM Thomas J. Watson Research Center, Yorktown Heights, New York 10598

and

Fred H. Pollak

Department of Physics, Brooklyn College of the City University of New York, Brooklyn, New York 11210
 (Received 21 July 1980; revised manuscript received 19 November 1980)

Electroreflectance measurements have been performed on the GaAs-Ga_{1-x}Al_xAs superlattice, and the observed structure has been related to interband transitions at different points of the Brillouin zone. For increasing x the energies of these transitions shift progressively to higher values with respect to those of bulk GaAs, indicating the effect of the superlattice potential on the band structure beyond the zone center. In contrast, similar shifts observed in In_{1-x}Ga_xAs-GaSb_{1-y}As_y only occur for $x, y > 0.2$, an anomaly arising from its unusual periodic potential.

PACS numbers: 71.25.Tn, 78.20.Jq

Recently, semiconductor superlattices of both GaAs-Ga_{1-x}Al_xAs and In_{1-x}Ga_xAs-GaSb_{1-y}As_y have been extensively studied. The formation of quantum states or subbands and their influence on electronic properties have been explored successfully by a variety of experiments.¹⁻⁸ These investigations, however, were confined to the subband structure in the vicinity of the fundamental gaps (Γ_{15v} - Γ_{1c}) of the host semiconductors. The basic question as to the general effect of the peri-

odic potential on the band structure remains unanswered.

In this Letter we report electrolyte electroreflectance (EER) measurements on GaAs-Ga_{1-x}Al_xAs (type-I) superlattices⁹ that provide the first observation of the superlattice effect on the band structure away from the Brillouin zone center. Of special significance is the observation of transitions associated with both E_1 and $E_1 + \Delta_1$ (L_{3v} - L_{1c}), and E_0 and $E_0 + \Delta_0$ (the lowest

direct gap and its spin-orbit-split component at Γ), which can be explained on the basis of a one-dimensional Krönig-Penney model treating the conduction and valence bands independently. In addition, we present similar EER measurements on $\text{In}_{1-x}\text{Ga}_x\text{As-GaSb}_{1-y}\text{As}_y$ (type-II) superlattices,⁹ involving the E_1 and $E_1 + \Delta_1$ transitions. The results also show the effect of the superlattice potential, but their quantitative interpretation requires considerations beyond the one-dimensional model.

The three superlattice configurations used for the present experiments are 110 periods of 77-Å(GaAs)-66-Å($\text{Ga}_{0.7}\text{Al}_{0.3}\text{As}$) (sample *A*); 110 periods of 50-Å(GaAs)-50-Å($\text{Ga}_{0.4}\text{Al}_{0.6}\text{As}$) (sample *B*); and 103 periods of 50-Å(GaAs)-50-Å(AlAs) (sample *C*), all prepared on (100) GaAs substrates. The electron concentration in all these samples, including a reference GaAs sample, is in the low 10^{16} cm^{-3} range. The EER measurements were carried out at room temperature in the energy range of 1.35–5.5 eV, with use of a technique described extensively in the literature.^{10, 11}

Shown in Fig. 1 is the EER spectrum of sample *C* in the energy range 1.35–2.1 eV. The structures below about 1.55 eV, where the superlattice is transparent, are attributed to Franz-

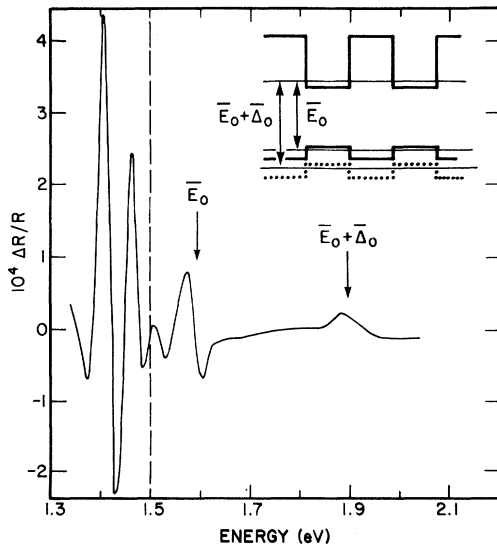


FIG. 1. Electrolyte electroreflectance spectrum of superlattice sample *C* (GaAs-AlAs) at room temperature in the vicinity of the fundamental gap and its spin-orbit-split component. Shown in the inset is the potential energy profile of this region for the GaAs- $\text{Ga}_{1-x}\text{Al}_x\text{As}$ superlattice system.

Keldysh oscillations of the E_0 gap of the GaAs substrate. Above 1.55 eV, two features labeled \bar{E}_0 and $\bar{E}_0 + \bar{\Delta}_0$ are observed here, and similarly in samples *A* and *B*. The transition energies, as listed in Table I, are obtained from the three-point method.^{12, 13} We associate the \bar{E}_0 transition with that between the ground states of heavy holes and electrons of the superlattice, and $\bar{E}_0 + \bar{\Delta}_0$ with that originating from the subbands of the spin-orbit-split potential.

We have calculated the energies of the ground states from the Krönig-Penney model, taking 1.43 eV and $1.43 + 1.52x$ eV as the lowest direct gaps of GaAs and $\text{Ga}_{1-x}\text{Al}_x\text{As}$ and $0.067m_0$ and $0.45m_0$ as the effective masses for electrons and heavy holes. We have calculated similarly the spin-orbit-split heavy-hole ground states using $\Delta_0 = 0.34$ eV for GaAs and $0.34 - 0.06x$ eV for $\text{Ga}_{1-x}\text{Al}_x\text{As}$.^{10, 14} The effective mass of the spin-orbit-split valence band, $0.155m_0$, was used.¹⁵ Results thus obtained for the various superlattice configurations are listed in parentheses in Table I. They are seen to compare very favorably with the experimental values of both \bar{E}_0 and $\bar{E}_0 + \bar{\Delta}_0$, demonstrating the superlattice effect on the band structure at the Γ point. Unlike previous investigations, our results were obtained at 300 K over the entire composition range, even where $\text{Ga}_{1-x}\text{Al}_x\text{As}$ becomes an indirect semiconductor.

In Fig. 2 we show the EER spectra in the range 2.5–5.5 eV for samples *A*, *B*, and *C*, as well as the reference GaAs. The E_1 and $E_1 + \Delta_1$ structures in GaAs are due to transitions along the Λ directions of the Brillouin zone. Samples *A*, *B*, and *C* exhibit corresponding features (\bar{E}_1 , $\bar{E}_1 + \bar{\Delta}_1$) at energies that shift monotonically to higher values as the Al composition is increased.

TABLE I. Energies (in eV) of the various transitions in the GaAs and superlattice samples. Calculated values, as explained in the text, appear in parentheses.

Sample	Transition			
	E_0	$E_0 + \Delta_0$	E_1	$E_1 + \Delta_1$
GaAs	1.43	1.77	2.92	3.14
<i>A</i>	\bar{E}_0	$\bar{E}_0 + \bar{\Delta}_0$	\bar{E}_1	$\bar{E}_1 + \bar{\Delta}_1$
	1.47 (1.49)	...	2.94 (2.96)	3.16
<i>B</i>	1.56 (1.57)	1.86 (1.92)	2.98 (3.02)	3.21
	<i>C</i>	1.59 (1.58)	1.89 (1.94)	3.03 (3.03)

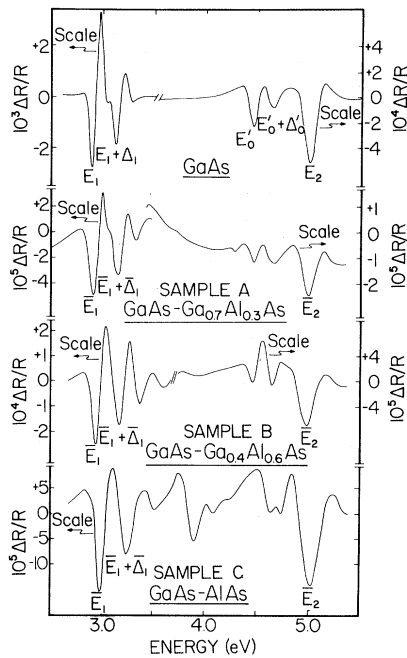


FIG. 2. Electroreflectance spectrum in the range 2.5–5.5 eV for superlattice samples A, B, and C, as well as the GaAs reference material.

We interpret this shift in terms of the formation of subbands from the E_1 and $E_1 + \Delta_1$ potential energy profiles in a manner analogous to that of the fundamental (E_0) gap region. We assume that along Λ the valence band of $\text{Ga}_{1-x}\text{Al}_x\text{As}$ is shifted rigidly with respect to that of GaAs; e.g., for AlAs the displacement is 0.23 eV. Hence, from a knowledge of the Γ - L conduction band separation of GaAs (0.29 eV),¹⁶ as well as the E_0 and E_1 gaps of GaAs and $\text{Ga}_{1-x}\text{Al}_x\text{As}$,¹⁷ the potential profile can be determined. Values for the L -point conduction and valence masses of GaAs along (100) are $0.11m_0$ and $0.29m_0$, respectively, as deduced from the expression $1/m_{100} = \frac{1}{3}m_l + \frac{2}{3}m_t$, where m_l and m_t are the longitudinal and transverse mass at the L point.¹⁶ Based on these considerations, the energies of the subband ground states, corresponding to \bar{E}_1 transitions, were calculated with use of the Krönig-Penney model, and are shown in parentheses in Table I. The good agreement between experimental and calculated values indicates the validity of the one-dimensional potential at both the Γ and the L points of the Brillouin zone. It also suggests that the effect of the superlattice potential on the band structure is manifested through the component of the effective mass tensor along the

superlattice direction.

Around 5 eV we observe the E_2 structure in GaAs and a feature labeled \bar{E}_2 in the superlattice samples. This EER peak shifts to somewhat higher energies with increasing x . An analysis similar to that performed for the \bar{E}_1 structure is difficult because of the more complex nature of E_2 .¹⁸ We also observe EER signals between 3.3 and 4.5 eV; e.g., sample B has structure at 3.4 and 3.6 eV. These features can be associated with the E_1 and $E_1 + \Delta_1$ transitions of the $\text{Ga}_{1-x}\text{Al}_x\text{As}$ bulk material¹⁷ but the origin of any observed shift is more ambiguous, as it can be due to small variations of x . Around 4.5 eV, the peaks can be associated with E_0' and $E_0' + \Delta_0'$ transitions. Since their energy positions are almost independent of x , it is difficult to ascertain their origins.

We have made similar investigations in $\text{In}_{1-x}\text{Ga}_x\text{As-GaSb}_{1-y}\text{As}_y$ superlattices ($x=y$) having a typical layer thickness of 50 Å, with emphasis on the E_1 and $E_1 + \Delta_1$ transitions. The results are drastically different from those just described for the type-I superlattice. For $x \leq 0.2$ sets of \bar{E}_1 and $\bar{E}_1 + \bar{\Delta}_1$ EER features are seen whose energies are in excellent agreement with those of the two host semiconductors. However, at $x > 0.2$ these energies rise abruptly above those corresponding to the hosts. For values of x (or y) approaching unity this shift decreases and eventually becomes zero for $x=y=1$ (GaAs). This situation is shown in Fig. 3, where we depict the E_1 and $E_1 + \Delta_1$ transition energies of the host materials $\text{In}_{1-x}\text{Ga}_x\text{As}$ and $\text{GaSb}_{1-y}\text{As}_y$ and the transition energies of the superlattices with similar alloy compositions.

In an attempt to explain these results, a similar Krönig-Penney model was used. Even though this model is not adequate for type-II superlattices at the Γ point, where a strong band interaction occurs, it is not unreasonable to use it at the L point, where the bands are far apart. The value for \bar{E}_1 in InAs-GaSb superlattices was calculated with use of a potential profile based on recent values of the energy separation between the L - and Γ -point conduction band minima^{19,20} in conjunction with the measured E_1 and $E_1 + \Delta_1$ for bulk GaSb and InAs. The calculated upshift of the \bar{E}_1 transition with respect to the homologous one in GaSb would be ~ 0.09 eV for 50-Å(InAs)-50-Å(GaSb) and ~ 0.14 eV for 33-Å(InAs)-33-Å(GaSb), which was also studied experimentally. Furthermore, if we assume a monotonic variation of the L -point valence and conduction bands with an in-

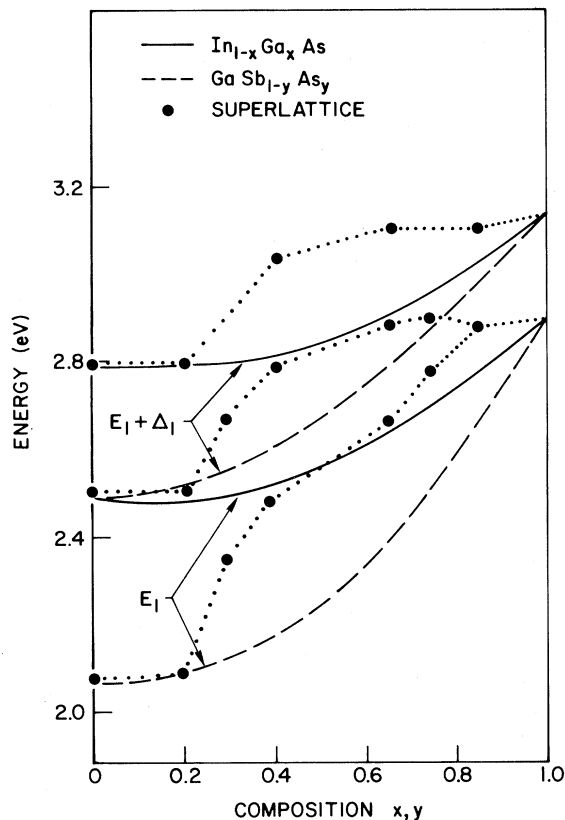


FIG. 3. Variation of the E_1 and $E_1 + \Delta$ transitions with composition for $\text{In}_{1-x}\text{Ga}_x\text{As-GaSb}_{1-y}\text{As}_y$ superlattices (closed circles) and for the $\text{In}_{1-x}\text{Ga}_x\text{As}$ (continuous line) and $\text{GaSb}_{1-y}\text{As}_y$ (discontinuous line) systems. The dots connecting the circles were drawn based on the line shapes of the observed spectra.

crease in x and y , then such a shift would decrease accordingly in a similar fashion. None of these predictions are consistent with experimental observations.

The observed different behavior of the \bar{E}_1 and $\bar{E}_1 + \bar{\Delta}_1$ structure in $\text{In}_{1-x}\text{Ga}_x\text{As-GaSb}_{1-y}\text{As}_y$ for values of x below or above 0.2 is of significance for the following reason. In superlattices having small x and y , the bottom of the conduction band of $\text{In}_{1-x}\text{Ga}_x\text{As}$ is located very close to or even below ($x=y \lesssim 0.3$) the top of the valence band of $\text{GaSb}_{1-y}\text{As}_y$, giving rise to a strong interaction between the two bands. Apparently the crossover of these two bands with increasing x and y affects dramatically the entire band structure of the superlattice.

The results presented in this work have demonstrated, in both the $\text{GaAs-Ga}_{1-x}\text{Al}_x\text{As}$ and the $\text{In}_{1-x}\text{Ga}_x\text{As-GaSb}_{1-y}\text{As}_y$ systems, the effect of the

superlattice potential away from the center of the Brillouin zone. The simple one-dimensional model, which has been successful in explaining almost all the observations reported, including our results for $\text{GaAs-Ga}_{1-x}\text{Al}_x\text{As}$ superlattices, is unable to account for the band structure of $\text{In}_{1-x}\text{Ga}_x\text{As-GaSb}_{1-y}\text{As}_y$ superlattices. It is hoped that this work will help to motivate fundamental considerations of the superlattice band structure beyond its current scope.

This work was supported by the U. S. Army Research Office, and by the U. S. Office of Naval Research under Contract No. N00014-78-C-0890.

(a)Permanent address: Institute of Physics, University of Uppsala, S-75121 Uppsala, Sweden.

¹L. Esaki and L. L. Chang, Phys. Rev. Lett. **33**, 495 (1974).

²H. Sakaki, L. L. Chang, G. A. Sai-Halasz, C.-A. Chang, and L. Esaki, Solid State Commun. **26**, 589 (1978).

³L. L. Chang, N. J. Kawai, G. A. Sai-Halasz, R. Ludeke, and L. Esaki, Appl. Phys. Lett. **35**, 939 (1979).

⁴N. J. Kawai, L. L. Chang, G. A. Sai-Halasz, C.-A. Chang, and L. Esaki, Appl. Phys. Lett. **36**, 369 (1980).

⁵R. Dingle, W. Wiegmann, and C. H. Henry, Phys. Rev. Lett. **33**, 827 (1974).

⁶R. Dingle, A. C. Gossard, and W. Wiegmann, Phys. Rev. Lett. **34**, 1327 (1975).

⁷R. Tsu, L. L. Chang, G. A. Sai-Halasz, and L. Esaki, Phys. Rev. Lett. **34**, 1509 (1975).

⁸G. A. Sai-Halasz, L. L. Chang, J.-M. Welter, C.-A. Chang, and L. Esaki, Solid State Commun. **27**, 935 (1978).

⁹G. A. Sai-Halasz, R. Tsu, and L. Esaki, Appl. Phys. Lett. **30**, 651 (1977).

¹⁰M. Cardona, K. L. Shaklee, and F. H. Pollak, Phys. Rev. **154**, 696 (1967).

¹¹F. H. Pollak, C. E. Okeke, P. E. Vanier, and P. M. Raccach, J. Appl. Phys. **49**, 4216 (1978).

¹²D. E. Aspnes and J. E. Rowe, Phys. Rev. Lett. **27**, 188 (1971).

¹³R. Wolf, W. Kühn, R. Enderlein, and H. Lange, Phys. Status Solidi (a) **42**, 629 (1977).

¹⁴A. Onton, in *Proceedings of the Tenth International Conference on the Physics of Semiconductors, Cambridge, Massachusetts, 1970*, edited by S. P. Keller, J. C. Hensel, and F. Stern, CONF-700801 (National Technical Information Service, Springfield, Va., 1970), p. 107.

¹⁵G. A. Sai-Halasz, A. Pinczuk, P. Y. Yu, and L. Esaki, Solid State Commun. **25**, 381 (1978).

¹⁶D. E. Aspnes, Phys. Rev. B **14**, 5331 (1976).

¹⁷O. Berolo and J. C. Woolley, *Can. J. Phys.* **49**, 1335 (1971).

¹⁸D. E. Aspnes and A. A. Studna, *Phys. Rev. B* **7**, 4605 (1973).

¹⁹P. Perrier, J. C. Portal, J. Galibert, and S. Aske-

nazy, in Proceedings of the Fifteenth International Conference on the Physics of Semiconductors, Kyoto, Japan, September 1980 (to be published).

²⁰J. R. Chelikowsky and M. L. Cohen, *Phys. Rev. B* **14**, 556 (1976).

Antiferromagnetic Ordering in the Organic Conductor *bis*-Tetramethyltetraselenafulvalene-Hexafluorophosphate [(TMTSF)₂-PF₆]

Kell Mortensen,^(a) Y. Tomkiewicz, T. D. Schultz, and E. M. Engler^(b)
IBM T. J. Watson Research Center, Yorktown Heights, New York 10598
(Received 12 January 1981)

The anisotropy in the static susceptibility of (TMTSF)₂-PF₆ has been investigated above and below the metal-insulator transition for a range of fields between 4 and 25 kOe. The results are consistent with the occurrence of an Overhauser antiferromagnetic transition to a spin-density-wave state with an easiest axis perpendicular to the stacks. Below the transition, evidence for a spin-flop transition is seen. Above the transition, evidence for a crossover, possibly from $n = 3$ to $n = 1$ spin behavior, is seen.

PACS numbers: 75.30.Gw, 71.30.+h, 75.30.Cr, 75.50.Ee

Recently, the new class of organic conductors (TMTSF)₂-X has generated extensive interest by exhibiting a number of physical properties different from those observed in chemically related compounds. In particular, (TMTSF)₂-PF₆, which is the first organic compound exhibiting superconductivity,¹⁻⁴ has been studied in detail. The superconducting state occurs under hydrostatic pressure above 6.5 kbar at temperatures near 1.2 K. At ambient pressure,⁵ (TMTSF)₂-PF₆ has been observed to undergo a metal-to-insulator (MI) transition in the temperature range 15–19 K, which is remarkably low compared with most other conducting organic charge-transfer salts. More recently, it has been suggested⁶ that there is also a magnetic transition at 11.5 K. In our samples, we see only one transition, at 11.5 K, in both the magnetic and transport properties. This transition is the subject of this paper.

Despite considerable experimental work, the nature of the MI transition in (TMTSF)₂-PF₆ and its relationship to the superconducting state remain a puzzle. Although the MI transitions occurring in the other known organic metals are believed to be associated with Peierls distortions, no indication of this type of distortion has been seen for (TMTSF)₂-PF₆ in diffuse x-ray scattering experiments⁷ down to 4 K. The magnetic and transport properties for $T \leq T_c$ have also proved

anomalous. At the transition temperature, Pedersen, Scott, and Bechgaard⁸ observed a significant reduction of the spin susceptibility, as measured by spin resonance in single crystals, whereas only minor effects were detected in the static susceptibility measured on a powdered sample.^{5,6} This is not what is expected from the opening of a Peierls gap. Additional experiments have shown^{9,10} that both the dc conductivity and spin paramagnetism are drastically affected by small electric fields (~ 10 mV/cm) at temperatures below T_c . These observations led to the speculation^{6,9} that a spin-density wave might be responsible for the MI transition.

To see if the MI transition is also a magnetic phase transition, we have studied the static magnetic susceptibility in detail, both parallel and perpendicular to the molecular stacking axis (a axis). The results presented in this paper provide the first *direct* evidence that antiferromagnetic ordering takes place in the MI transition. We observe an anisotropic susceptibility at small fields (~ 4 kOe) for $T < T_c$, an apparent spin-flop transition in somewhat larger fields transverse to a , and the disappearance of anisotropy effects with increasing fields. That the transition is magnetic is in accord with the argument of Scott, Pedersen, and Bechgaard that if there is only one transition, it is magnetic.